

Experimental investigation of reinforced concrete columns retrofitted with polyester sheet

Chunho Chang^{1a}, Sung Jig Kim^{*2}, Dongbyung Park^{1b} and Sunghun Choi^{1c}

¹Department of Civil Engineering, Keimyung University, Dalseo, Daegu, 704-701, Korea

²Department of Architectural Engineering, Keimyung University, Dalseo, Daegu, 704-701, Korea

(Received January 25, 2013, Revised July 23, 2013, Accepted November 24, 2013)

Abstract. This paper experimentally investigates the seismic performance of RC columns retrofitted with Super Reinforcement with Flexibility (SRF), which is a polyester fiber reinforced polymer. A total of three specimens with a scale factor of 1/2 were constructed and tested in order to assess the structural behavior of the retrofitted RC columns. One specimen was a non-seismically designed column without any retrofit, while others were retrofitted with either one or two layers of the polyester belt with urethane as the adhesive. Static cyclic testing with a constant axial load was conducted to assess the seismic performance of the retrofitted RC columns. It is concluded that the SRF retrofitting method increases the strength and ductility of the RC columns and can also impact on the failure mode of the columns.

Keywords: seismic retrofit; reinforced concrete column; SRF(Super Reinforcement with Flexibility); shear failure

1. Introduction

Many of recent researches to reduce seismic vulnerability of existing structures and improve their performance during earthquakes have focused on seismic retrofit by modifying structures and structural components or adding additional elements. In past earthquakes (e.g., the Loma Prieta (1989) and Northridge earthquakes (1994) in California and the Hyogo-ken Nanbu earthquake (1995) in Kobe, Japan), shear damage and failure of concrete columns was prevalent. Previous investigations have attributed the observed failures to inadequate flexural ductility and insufficient shear capacity of reinforced concrete (RC) columns which are mostly caused by insufficient transverse confinement and low aspect ratio (i.e., ratio of shear span to depth). Thus, retrofitting strategies that address column deficiencies often aim to enhance the confinement for concrete columns in order to provide an increased ductility capacity and/or improved shear strength. Some examples of such retrofitting methods include steel jacketing and steel plates or fiber (carbon or glass) reinforced plastic (FRP) sheets wrapped around the column.

*Corresponding author, Assistant Professor, E-mail: sungjigkim@gmail.com

^a Associate Professor, E-mail: chunho@gw.kmu.ac.kr

^b Graduate Student, E-mail: pdb4217@kmu.ac.kr

^c Graduate Student, E-mail: cas_per@nate.com

The use of fiber composite materials in seismic retrofit applications to columns has grown rapidly since the 1990s due to its effectiveness in strengthening the structural members of existing buildings which cannot satisfy current design demands (Yamamoto 1992, Seible *et al.* 1995, Saadatmanesh *et al.* 1997, Bournas *et al.* 2009, Perrone *et al.* 2009, ElSouri and Harajli 2011, Gu *et al.* 2011, Wang *et al.* 2011, Park and Yoo 2013). Compared to the steel plate bonding method, the FRP strengthening method has advantages such as easy installation due to the light weight, chemical resistance and lower labor cost. The Carbon Fiber Reinforced Polymer (CFRP) retrofit method enhances both stiffness/strength and ductility of structural members due to the high strength and stiffness of CFRP materials (Gao *et al.* 2005). However, some experimental research has reported that peeling and shear cracks at the end of the plate which caused premature failure of RC members with FRP plates (Bakis *et al.* 2002).

More recently, a new strengthening method for RC columns which uses polyester fiber was developed in Japan to improve axial loading capacity under large lateral deformation and to prevent the collapse of structures under severe seismic loadings (Kabeyasawa *et al.* 2002, Kabeyasawa *et al.* 2004, Kim *et al.* 2012). This method is called the Super Reinforced with Flexibility (SRF) method and the important characteristics of the SRF material are its toughness, durability, heat resistance and flexibility. Static tests conducted by Kabeyasawa *et al.* (2002) and Kabeyasawa *et al.* (2004) showed that the columns strengthened by the SRF method can carry relatively high gravity loads under drift ratios of more than 10%, while the non-retrofitted specimens suffered shear failure at small drift ratios, resulting in loss of axial load carrying capacity. Kim *et al.* (2012) conducted shake table tests for two eccentric wall-frame specimens with identical section details and material properties but with one of RC column specimens retrofitted using the SRF method. This research demonstrated that the retrofitted column showed stable hysteretic relations without any considerable damage while the non-retrofitted columns experienced severe shear strength deterioration and compression failure due to the axial load along with inelastic load reversal and final collapse. When comparing with the conventional FRP retrofit methods, a series of tests described above showed that the SRF retrofit method is more effective for improving post-peak behavior and axial load carrying capacity of columns at large deformation although considerable enhancement of the initial stiffness and ultimate strength cannot be expected. However, since the experimental database and parametric study considering various retrofitting strategies of the SRF method are limited due to its relatively recent development, more experimental and analytical studies could be urgently required to generalize and apply this method.

In this paper RC columns retrofitted by the SRF method were constructed and tested to investigate the seismic performance of retrofitted RC columns. A total of three specimens with a scale factor of 1/2 were constructed and tested in order to assess the structural behavior of the retrofitted RC columns. One specimen was a non-seismically designed column without any retrofit, while the others were retrofitted with the polyester fiber belt with urethane as the adhesive. In order to investigate the effect of the number of the polyester belt layers on the column behavior, the retrofitted RC columns were wrapped by either one or two layers of the polyester belt. First, detailed aspects of the experimental framework including test specimen design, retrofitting method, and test setup are described. Next, observations and implications of the experimental results gathered from the three cyclic tests are provided. The effect of the SRF retrofitting method on the overall response of the column is discussed through the comparison of global response, damage status, shear strength, and energy dissipation.

2. Experimental program

2.1 Test specimen

In order to assess the seismic behaviour of RC column retrofitted with the SRF method, half scale models of a prototype column were constructed and tested. As shown in Fig. 1, the section of the test specimens is 400×400 mm with 16-D22 longitudinal rebars and D10 stirrups. The spacing of the transverse rebars is 220 mm. Thus, the longitudinal rebar ratio is 2.90% and the volumetric ratio of the transverse rebar is 0.39%, which indicates the low confinement. The concrete strength is 31.8 MPa while the yield strengths of longitudinal and transverse rebars are 388.6 MPa and 380.9 MPa, respectively. Three specimens were simultaneously constructed with a height of 1400 mm, resulting in an aspect ratio of 3.5 as shown in Fig. 1. The stiff end cap beam at the bottom of the column has length, depth, and width of 1500 mm, 700 mm, and 800 mm, respectively, and is designed conservatively to avoid significant deformation and development of cracks during the tests. The axial loading blocks with 2000×2000×1100 mm were constructed in order to apply the axial load to the test specimen as shown in Fig. 2.

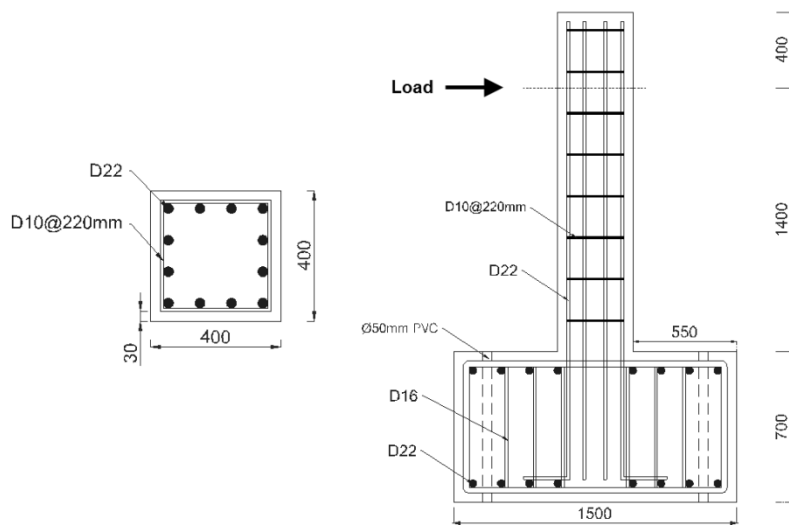


Fig. 1 Section and elevation of the specimen (unit: mm)



Fig. 2 Axial loading block

2.2 Retrofitting method and test setup

As described previously, the SRF retrofitting method was utilized to provide the enhanced ductility and strength to RC column under seismic loading. The polyester belt and urethane adhesive used in the SRF strengthening method are shown in Fig. 3. The thickness and width of the polyester belt are 2.5 mm and 100 mm, respectively. The tensile strength and elastic modulus of the belt are 423.55 MPa and 1659.36 MPa, respectively. The distinctive characteristic of the polyester belt relative to other retrofitting materials such as FRP is that the polyester belt can carry only tension and hardly ever resist compression. Thus, it exerts very high and ductile resistance in the tensile direction while very low compressive stress is generated in the polyester belt. Additionally, the polyester belt and urethane adhesive are much more flexible than concrete and steel and thus, its adherend, the concrete surface, is not damaged due to the fracture or peeling of strengthening materials, which can be observed from stiff and strong strengthening materials used in the FRP retrofit method (Kim *et al.* 2012).



Fig. 3 SRF belt and urethane adhesive



Fig. 4 Retrofitting process

Table 1 Specimen IDs and properties of retrofitting materials

Specimen	No. of Layer	Thickness
NRC		N.A.
SRF-1	1	2.5 mm
SRF-2	2	5 mm

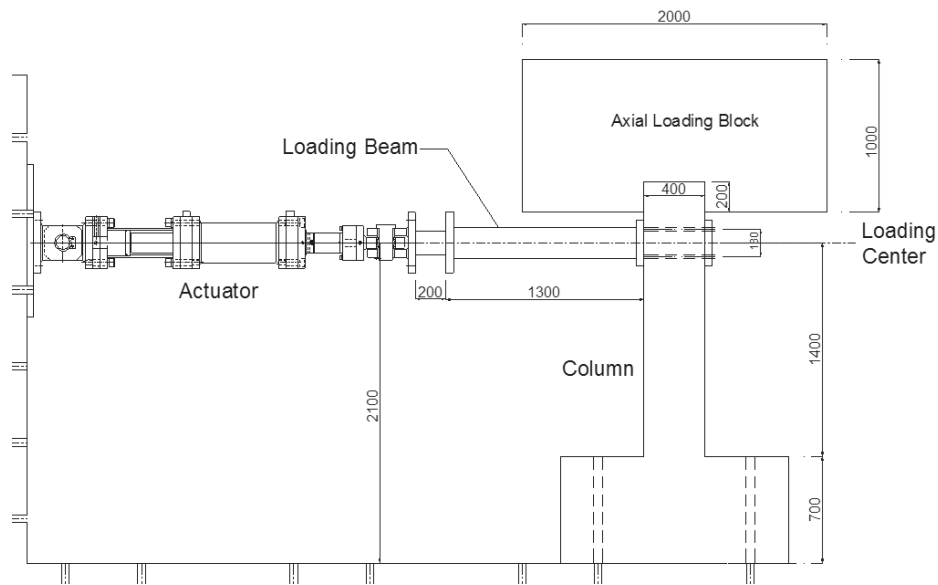


Fig. 5 Testing setup (unit: mm)

As listed in Table 1, a non-retrofitted RC column (NRC) and two RC columns retrofitted with the SRF method were tested. The second specimen (SRF-1) was retrofitted with a layer of polyester belt. In order to investigate the effect of the number of the polyester belt layers on the structural behavior, the third specimen (SRF-2) was retrofitted with two layers of the polyester belt, where the second layer was wrapped in the opposite direction as the first one. The construction process of SRF retrofitting method is shown in Fig. 4. Fig. 5 illustrates the overview of test setup for the test specimens. During each test, 24 channels of data were recorded continuously through a traditional DAQ acquisition.

3. Experimental results and observations

3.1 Loading protocol

Fig. 6 shows the applied lateral displacement history for the cyclic tests with constant axial load. All testing specimens were subjected to the axial compression of 103.56 kN by utilizing the axial loading block shown in Fig. 2, which was designed to corresponding to 2% of the axial capacity of the specimen. The imposed displacement history included three cycles at each displacement level up to a drift ratio of 1% and two cycles at each displacement level after 1%. The imposed

displacement pattern of two or three cycles provides an indication of the strength degradation characteristics. From the analytical prediction of the non-retrofitted column, the magnitude of the third drift ratio level was determined as 0.75% which was thought to develop the inelastic behavior of the RC column. The magnitude of the subsequent displacement level after 1% was determined with an increment of 0.5% and the final stage was determined considering the damage status of the tested specimen.

3.2 Test of non-retrofitted RC column

During the first cycle in the simulation with lateral drift ratio of 0.25%, flexural cracks were observed at the bottom of the column. Diagonal shear cracks were observed when the lateral drift ratio reached 1%. Also, inclined cracks occurred on the front face of the column along the height at a drift ratio of 2.44%. A maximum force of 216.71 kN was observed. When the lateral drift ratio reached about 4%, severe diagonal cracks and spalling of the concrete cover were observed, as shown in Fig. 7. The concrete cover below the middle of the specimen was completely spalled out. Severe damage was observed in the core concrete with diagonal cracks and a deep angle of about 60° . The lateral force was recorded to be 68.15 kN, which was 31.45% of the maximum force

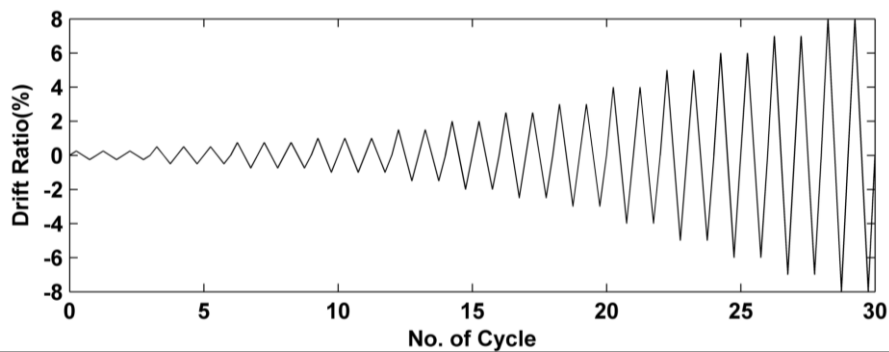


Fig. 6 Loading protocol

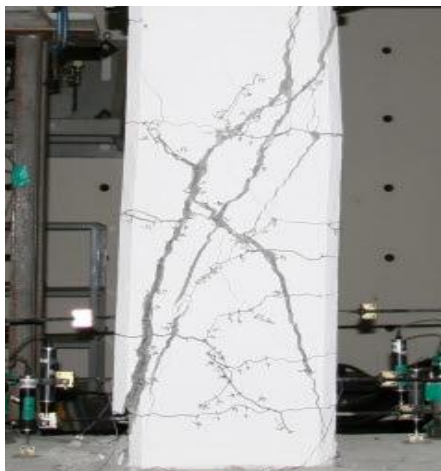


Fig. 7 Damage during the test, NRC

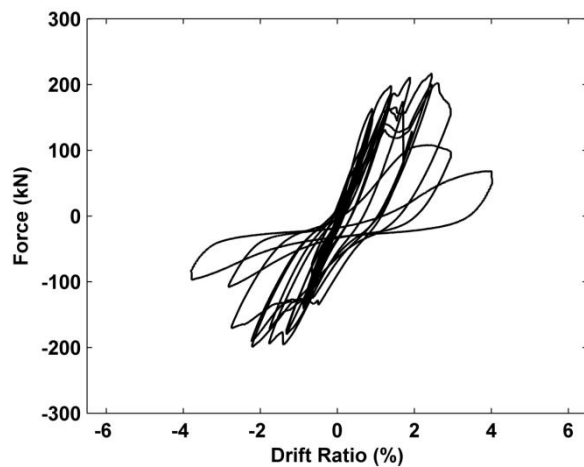


Fig. 8 Displacement and force, NRC

measured during the simulation. Therefore, the test had to be stopped due to the loss of resistance.

Fig. 8 shows the displacement and force relationship recorded during the test. The maximum force of NRC was 216.71 kN and the lateral force was significantly reduced after a drift ratio of approximately 4%. As shown in this figure, strength and stiffness degradation, and pinching of the hysteresis loops were observed, which indicate that typical behaviour of the shear failure mode.

3.3 Test of RC columns retrofitted with the SRF method

The specimens retrofitted with the polyester belt were also tested by applying a cyclic load identical to that of the specimen NRC. Since the polyester belt was wrapped around the column as illustrated in Fig. 4, the crack development on the surface of both columns could not be captured during the test. However, flexural cracks were observed at the joint between the column and bottom cap as shown in Fig. 9. These cracks in the specimen SRF-1 were developed when the drift ratio reached 1%, while flexural cracks in the specimen SRF-2 were captured at the drift ratio of about 3%. During the test with the specimen SRF-2, a significant bottom slip occurred and the actuator reached a displacement close to its limit in the negative direction as the input displacement level increased. Thus, the actuators could not follow exactly the input command and the desired displacement could not be achieved in the negative direction. Both specimens showed the typical flexural behaviour and reached up to a 6% drift ratio. Since no significant strength degradations were observed, it was decided to stop the tests at the drift ratio of 6%. At the final peak, the specimens SRF-1 and SRF-2 were able to carry lateral forces of 253.78 kN and 279.86 kN, respectively, which were maximum values during each test.



Fig. 9 Damage during the test, Retrofitted columns

After completing both tests, the polyester belt was removed from the specimens to investigate the damage included in the specimens. As shown in Fig. 10, flexural cracks at the bottom of the specimens were observed. However, the damage of both specimens was significantly reduced when compared to those of the specimen NRC. As illustrated in Fig. 10, a number of flexural cracks in the specimen SRF-1 were observed, while cracks in the specimen SRF-2 were limited.

Fig. 11 illustrates the comparison of the force-displacement relationship for the specimens

either NRC and SRF-1 or NRC and SRF-2. The maximum lateral forces of the specimens SRF-1 and SRF-2 were increased by 17.10% and 29.14%, respectively when compared to that of the specimen NRC. As described previously, the desired displacement for the specimen SRF-2 could not be achieved due to the significant slip at the bottom of the specimen as shown in Fig. 11(b). In contrast with the specimen NRC, the specimens SRF-1 and SRF-2 show flexural behaviour and a substantial increase in energy dissipation.



Fig. 10 Damage after tests, Retrofitted columns

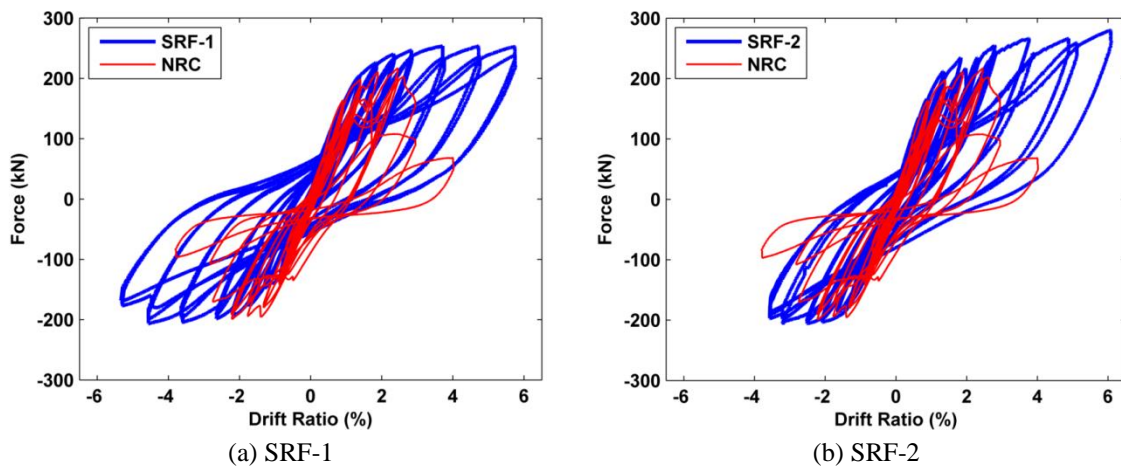


Fig. 11 Displacement and force, Retrofitted columns

4. Interpretation of experimental observation

Experimental results from the three specimens are compared in Table 2. Fig. 12(a) shows the comparison of the force-displacement relationship of each test specimen. The envelope curves for all specimens were estimated as shown in Fig. 12(b). Since the displacement of the specimen SRF-2 in the negative direction was not achieved as mentioned before, the envelope curves shown in Fig. 12(b) presents only the positive direction in order to clearly compare the behavior of the

test specimens. Additionally, the shear strength of the specimen NRC is evaluated by employing methods considering axial force provided by ACI 318-11 and Priestley *et al.* (1994). The shear strength model by Priestley *et al.* (1994) adopts a realistic shear crack inclination and accounts for the decrease of shear strength with the degradation of concrete due to inelastic deformations, resulting in the small scatter from real test results. This model assumes that the strength consists of three independent components as following

$$V_n = V_c + V_s + V_p \tag{1}$$

V_c is the contribution of concrete shear resisting mechanism considering the instantaneous displacement or curvature ductility, V_s is the contribution of the truss mechanism provided by shear reinforcement, and V_p represents the shear resistance of the arch mechanism, provided by axial force. V_c is given by

$$V_c = k\sqrt{f'_c}A_e \tag{2}$$

where, $A_e (= 0.8A_{gross})$ is the effective shear area and k depends on the instantaneous displacement or curvature ductility, the system of units (MPa or psi). The contribution of transverse reinforcement to shear strength is based on the truss mechanism using a 30° angle of inclination between the shear cracks and the vertical column axis. Thus, the contribution of transverse reinforcement, V_s for the rectangular column can be calculated by

$$V_s = \frac{A_v f_y D'}{s} \cot 30^\circ \tag{3}$$

where, A_v is the total transverse reinforcement area per layer and D' is the distance between centers of the peripheral hoop in the direction parallel to the applied shear force. The shear strength enhancement by axial force is considered to result from an inclined compression strut given by

$$V_p = P \tan \alpha = \frac{D - c}{2a} P \tag{4}$$

Table 2 Comparison of peak responses

Target Drift Ratio (%)	NRC			SRF-1			SRF-2		
	Displ. (mm)	Drift (%)	Force (kN)	Displ. (mm)	Drift (%)	Force (kN)	Displ. (mm)	Drift (%)	Force (kN)
0.25	3.09	0.22	45.40	2.67	0.19	52.17	3.01	0.22	58.35
0.50	6.25	0.45	73.74	5.83	0.42	91.69	6.01	0.43	99.43
1	12.63	0.90	163.76	12.30	0.88	155.43	12.14	0.87	166.02
2	26.39	1.89	211.12	25.65	1.83	226.13	25.69	1.84	234.66
2.5	34.20	2.44	216.71	32.74	2.34	240.25	32.21	2.30	234.85
4	54.87	3.92	68.15	52.02	3.72	253.78	52.41	3.74	266.53
6				80.08	5.72	252.41	84.90	6.06	279.86

where D is section depth or diameter, c is the compression zone depth which can be determined from flexural analysis, and a is the shear span which is $L/2$ for a column in reversed bending and L for a cantilever column.

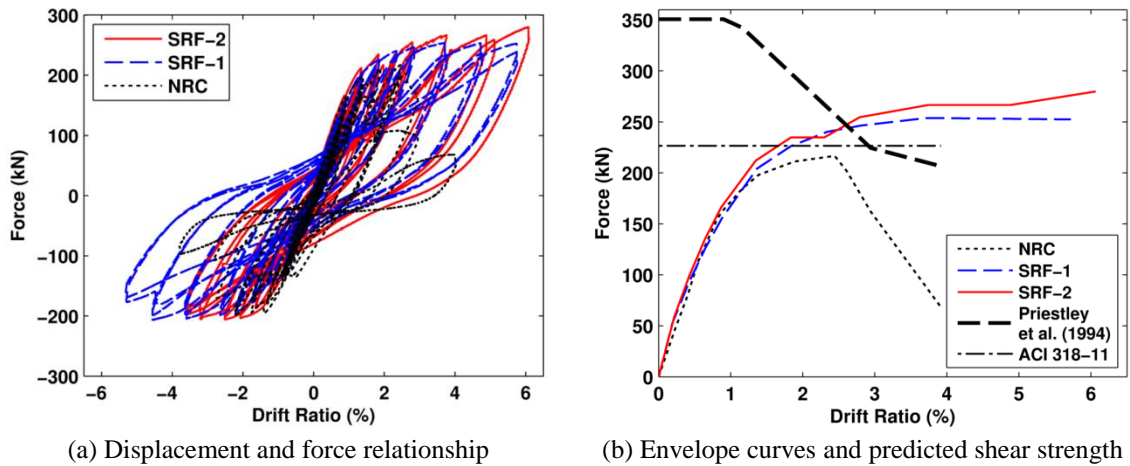


Fig. 12 Comparison of test results

The obtained experimental data are used to estimate shear strength of the specimen NRC. The displacement ductility, instead of the curvature ductility, is used to estimate the shear strength contribution of concrete (V_c) in the Priestley approach. This is because some curvature measuring instruments reached their limits during the experiments. Additionally, the number of curvature measuring instruments installed on the specimen NRC is insufficient to estimate the curvature. The shear capacity is estimated at each peak loading step and compared with the measured shear demand to investigate the overall trend and represents in Fig. 12(b).

The maximum force of the specimen NRC was 216.71 kN with a drift ratio of 2.44%, after which the lateral force was significantly reduced. Compared to the maximum strength, the strength of the specimen NRC at the drift ratio of 3.92% was reduced by 68.55%, indicating shear dominant behavior with significant strength degradation. The strength degradation of the specimen NRC can be easily found from the relationship between the lateral displacement and force shown in Fig. 12(a). In contrast to the specimen NRC, the specimens retrofitted with the SRF material did not experience any strength degradation. As shown in Fig. 12(a), the lateral forces of both SRF-1 and SRF-2 slightly increased as the number of loading cycles increased, resulting in flexural behavior. The maximum force of specimens SRF-1 and SRF-2 are 253.78 kN and 279.86 kN, respectively. When retrofitted with the SRF material, the maximum force of the specimen increased by 17.10% for one layer and 29.14% for two layers of the polyester belt when compared with that of the specimen NRC. Additionally, the maximum force of SRF-2 increased up to 10.28% when compared to that of SRF-1. Thus, as the number of layers of the SRF materials increased, the strength also increased.

Fig. 12(b) shows the envelope curves of test specimens and comparison with the shear strengths estimated by ACI 318-11 and Priestley approach for the specimen NRC. The estimated shear capacities at the drift ratio of 3% by ACI 318-11 and Priestley approach are 226.5 kN and 224.5

kN, which are close to the maximum shear demand (216.71 kN) of the specimen NRC with errors of -4.52% and -3.59%, respectively. However, the estimated shear capacities are smaller than shear demands of specimens SRF-1 and SRF-2. The measured shear forces of specimens SRF-1 and SRF-2 are approximately 11% and 20% larger than the estimated shear capacity.

Fig. 13 presents the absorbed energy per cycle calculated from the measured displacement and force during the test. This figure clearly indicates that the SRF retrofitting method can enhance the energy absorption of an RC column, which can lead to the ductile behavior. The accumulated energy up to 19 cycles of the specimens NRC, SRF-1, and SRF-2 are 26.40 kN·m, 31.71 kN·m, and 29.37 kN·m, respectively, which is not a substantial difference. However, the specimens retrofitted with the SRF material survived beyond 20 cycle and the accumulated energy up to 24 cycles of the specimens SRF-1 and SRF-2 are 74.98 kN·m and 70.41 kN·m, respectively. Thus, a total of the accumulated energy of the specimens SRF-1 and SRF-2 increased by 184.0% and 166.7 %, respectively. Therefore, it is concluded that the SRF retrofitting method can significantly affect the behavior and failure mode of an RC column.

As described above, taking into account the measured lateral force, the shear strength estimated using the realistic predictive approach, the observed damage status and failure mode of the columns, and the accumulated energy, it is concluded that the SRF retrofitting method can reduce seismic vulnerability of the RC column without seismic details.

The Mid-America Earthquake Center program Zeus-NL was utilized to analyze the behavior of the test specimens. Zeus-NL is an inelastic fiber analysis package which was specifically developed for earthquake engineering applications (Elnashai *et al.* 2004). To consider the polyester belt, composite section shown in Fig. 14(a) is employed in this study. The material of the polyester belt is modeled with frp1 provided in Zeus-NL. The modeling approaches of reinforced-concrete behavior in the most Finite Element analysis program allow a reasonable prediction of flexural response with adequate accuracy. However, the determination of shear strength and deformation characteristics is still challenging. Thus, in this study the columns are modeled with a shear spring in parallel with an inelastic beam element as shown in Fig. 14(b) by employing the approach by Lee and Elnashai (2001) in order to account for shear deformation. The primary curve of the shear spring is defined by a quadrilinear symmetric relationship that accounts for the cracking, yielding, and ultimate states, as shown in Fig. 14(b). The force-displacement of each specimen shown in Fig. 12(a) was compared with results from the Zeus-NL model without shear spring and the primary curve for each specimen is defined.

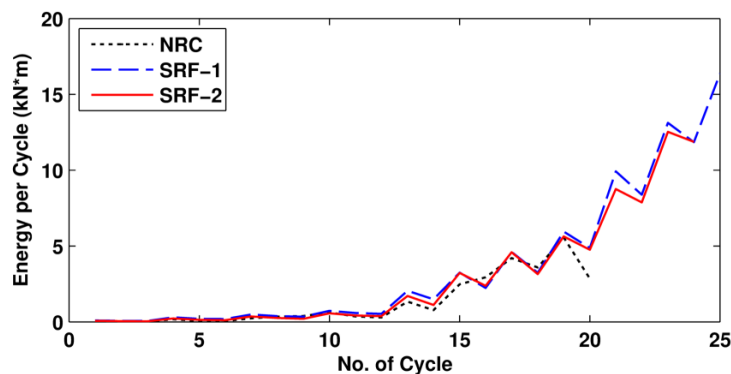
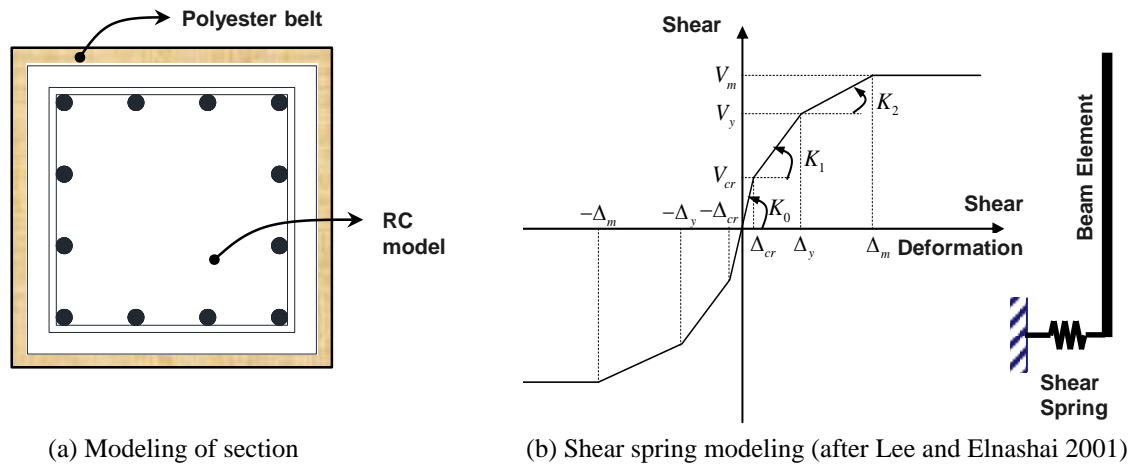


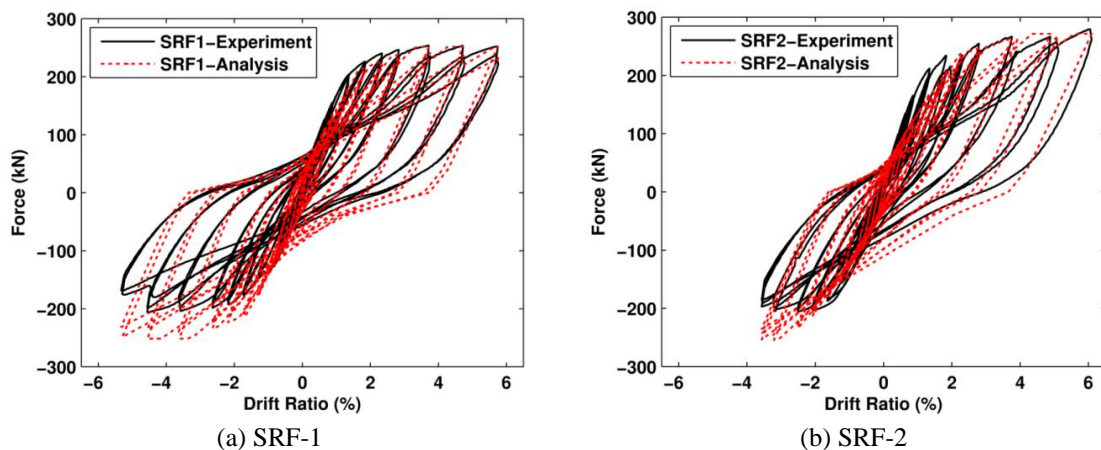
Fig. 13 Energy absorption at each cycle



(a) Modeling of section

(b) Shear spring modeling (after Lee and Elnashai 2001)

Fig. 14 Modeling approach of test specimens



(a) SRF-1

(b) SRF-2

Fig. 15 Comparison with analytical results

As illustrated in Fig. 15, analytical results were compared with experimental data of both specimens SRF-1 and SRF-2. Although the analytical result shows slightly larger energy dissipation capacity, a good agreement in both strength and stiffness in the positive direction is observed. However, the evaluated strengths from analytical results are larger than those of test results. This is because the primary curve of the shear spring is determined accounting for the positive direction of the envelope curve due to the limit of experimental data. In addition, pinching of the hysteresis loops observed in the experimental data is reflected in the analysis.

5. Conclusions

In this paper, the seismic performance of RC columns retrofitted by Super Reinforcement with Flexibility (SRF) was experimentally evaluated by employing cyclic static tests. The most important findings are summarized below.

The non-retrofitted specimen, NRC experienced brittle shear failure, while the specimens retrofitted with the SRF method showed ductile behavior. From the overall force-displacement relationship, the strength of specimen NRC showed significant strength degradation, while that of specimens retrofitted with the SRF method increased marginally. The lateral force of the retrofitted specimen increased by 17~ 30%. The measured shear forces of the specimens retrofitted with SRF are 11% ~ 20% larger than the shear capacity of the specimen NRC estimated by the ACI code and the realistic predictive approaches. Compared to the specimen NRC, a total of the accumulated energy of the specimens retrofitted with the SRF method substantially increased by up to 184.0%.

Hence, considering observations from these tests described above, it is clearly shown that the retrofitting method using the SRF method improves the seismic performance of RC columns and can ultimately dictate the failure mode.

Acknowledgments

The work presented in this paper was supported by the Daegu Technopark R&D in 2011.

References

- ACI (2011), *Building code requirements for structural concrete (ACI 318-11) and commentary (ACI 318R-11)*, American Concrete Institute.
- Bakis, C.E., Bank, L.C., Brown, V.L., Cosenza, E., Davalos, J.F., Lesko, J.J., Machida, A., Rizkalla, S.H. and Triantafillou, T.C. (2002), "Fiber-reinforced polymer composites for construction - state-of-the-art review", *J. Compos. Constr.*, **6**(2), 73-87.
- Bournas, D.A., Triantafillou, M., Zygouris, K. and Stavropoulos, F. (2009), "Textile-reinforced mortar versus FRP jacketing in seismic retrofitting of RC columns with continuous or lap-spliced deformed bars", *J. Compos. Constr.*, **13**(5), 360-371.
- Elnashai, A.S., Papanikolaou, V. and Lee, D. (2004), "Zeus NL - a system for inelastic analysis of structures", *Mid-America Earthquake Center CD-Release 04*, University of Illinois at Urbana-Champaign.
- ElSouri, A.M. and Harajli, M.H. (2011), "Seismic repair and strengthening of lap splices in RC columns: carbon fiber-reinforced polymer versus steel confinement", *J. Compos. Constr.*, **15**(5), 721-731.
- Gao, B., Leung, C. and Kim, J. (2005), "Prediction of concrete cover separation failure for RC beams strengthened with CFRP strips", *Eng. Struct.*, **27**, 177-189.
- Gu, D., Wu, G., Wu, Z. and Wu, Y. (2011), "Confinement effectiveness of FRP in retrofitting circular concrete columns under simulated seismic load", *J. Compos. Constr.*, **14**(5), 531-540.
- Kabeyasawa, T., Tasai, A. and Igarashi, S. (2002), "An economical and efficient method of strengthening reinforced concrete columns against axial load collapse during major earthquake", *The Third Workshop on Performance-based Engineering on Reinforced Concrete Building Structures*, Seattle, WA. PEER Report 2002/02, 371-384.
- Kabeyasawa, T., Tasai, A. and Igarashi, S. (2004), "Test and analysis of reinforced concrete columns strengthened with polyester sheet", *Proceedings of 13th World Conference on Earthquake Engineering*, Vancouver, B.C., Canada, August.
- Kim, Y., Kabeyasawa, T. and Igarashi, S. (2012), "Dynamic collapse test on eccentric reinforced concrete structures with and without seismic retrofit", *Eng. Struct.*, **34**, 95-110.
- Lee, D.H. and Elnashai, A.S. (2001), "Seismic analysis of RC bridge columns with flexure-shear interaction", *J. Struct. Eng.*, **127**(5), 546-553.
- Park, J.W. and Yoo, J.H. (2013), "Axial loading tests and load capacity prediction of slender SHS stub columns strengthened with carbon fiber reinforced polymers", *Steel Compos. Struct.*, **15**(2), 131-150.

- Perrone, M., Barros, J. and Aprile, A. (2009), "CFRP-based strengthening technique to increase the flexural and energy dissipation capacities of RC columns", *J. Compos. Constr.*, **13**(5), 372-383.
- Priestley, M.J.N., Verma, R. and Xiao, Y. (1994), "Seismic shear strength of reinforced concrete columns", *J. Struct. Eng. - ASCE*, **120**(8), 2310-2329.
- Saadatmanesh, H., Ehsani, M.R. and Jin, L. (1997), "Repair of earthquake-damaged RC columns with FRP wraps", *ACI Struct. J.*, **94**(2), 206-215.
- Seible, F., Hegemier, G.A., Priestley, M.J.N. and Innamorato, D. (1995), "Developments in bridge column jacketing using advanced composites", *Proceedings of the National Seismic Conference on Bridges and Highways*, San Diego, December.
- Sheikh, S.A. (2002), "Performance of concrete structures retrofitted with fibre reinforced polymers", *Eng. Struct.*, **24**(7), 869-879.
- Wang, Y., Ma, Y. and Wu, H. (2011), "Reinforced high-strength concrete square columns confined by aramid FRP jackets. Part I: Experimental study", *Steel Compos. Struct.*, **11**(6), 455-468.
- Yamamoto, T. (1992), "FRP strengthening of RC columns for seismic retrofitting", *Proceedings of the 10th World Conference on Earthquake Engineering*, Madrid, Spain, July.

CC